

# Characteristics of adsorption isotherm and kinetic study for newly prepared Co<sup>2+</sup>-imprinted polymer linkage with dipicolinic acid

N F Yusof<sup>1</sup>, F S Mehamod<sup>2</sup>, M A Kadir<sup>2</sup> and F B M Suah<sup>3</sup>

<sup>1</sup>School of Fundamental Science, Universiti Malaysia Terengganu, 21030 Kuala Nerus, Malaysia.

<sup>2</sup>Advanced Nano Materials Research Group, School of Fundamental Science, Universiti Malaysia Terengganu, 21030 Kuala Nerus, Malaysia.

<sup>3</sup>School of Chemical Sciences, Universiti Sains Malaysia (USM), 11800 Minden, Pulau Pinang, Malaysia.

Corresponding author emails: fshimal@umt.edu.my

**Abstract.** Co<sup>2+</sup>-complex imprinted polymer (Co-IIP) was prepared by ionic imprinting technology for selective removal of Co<sup>2+</sup> ions from aqueous solution. Co<sup>2+</sup> which act as a template ion established a coordination linkage with dipicolinic acid before being copolymerized with functional monomer (methacrylic acid) in the presence of cross-linker (ethylene glycol dimethacrylate) and initiator (2,2'-azobisisobutyronitrile). The surface features and functional groups present in imprinted polymer were characterized by scanning electron micrograph and infrared spectra. The non-imprinted polymer (NIP) was produced simultaneously to serve as controlled polymer. From the isotherm study, adsorption of Co<sup>2+</sup> ions by ion imprinted polymer (IIP) followed Langmuir isotherm model, which indicates the sorption can be described by monolayer adsorption by give the maximum adsorption capacity was 19.57 mg g<sup>-1</sup>. This value was comparable to the experimental value which was 18.48 mg g<sup>-1</sup> and better affinity compared to NIP. The adsorption kinetics fit a pseudo-second-order and adsorption equilibrium time was around 30 minutes. The present work has successfully synthesized Co-IIP particles with good potential in recognition of Co<sup>2+</sup> ions.

## 1. Introduction

Molecular imprinting is a study of molecular recognition which is widely exploited in a numbers of applications. It is a technique for making selective binding sites towards the analyte (template) in polymeric matrices. The concept of molecular imprinting is analogous to lock and key hypothesis proposed by Emil Fischer, a Nobel laureate who explained enzyme-substrate interaction. It was early attributed by Polykov in 1930s to investigate the silica matrix for various additives extraction and it was continued develop by Linus Pauling in 1940s. This discovery had resulted in intensive research on imprinting technology. The imprinting process can be illustrated into three main stages [1]; 1) mixing the functional monomer with the target molecule or template in the suitable porogen according to predetermined ratio. Pre-polymerization occurs between template and monomer via covalent or noncovalent bonding; 2) the growing polymer chain will be created as the free radical polymerization



takes part in the solution. Cross-linkers are added and polymerize to achieve highly cross-linked polymers. The structure of adducts will freeze and fix around the template molecule; 3) lastly, the removal of template from the polymer thus leaves the specific binding site corresponding to the template molecule. Due to the complementarity of recognition sites to template in terms of size, shape and chemical functionality orientations as well as contribution from environment, rebinding of subsequent template is thus allowed.

Rebinding recognition in imprinting involves the sorption process between template molecule and polymer. When this molecular species is in contact with a solid surface of polymer, there will be an equilibrium establishment. In the liquid phase, monitoring the coverage of the surface in relation to the concentration at a fixed temperature is described as adsorption isotherm. The equilibrium adsorption isotherm is an important assessment for the theoretical determination design of adsorption system. Ion imprinted polymers (IIP) is a branch of molecular imprinting study by changing the template molecule to inorganic ions. Commonly, metal ion is dominant used as template molecule for imprinting purpose. The first ion imprinting was introduced by Nishide and co-workers by cross-linked poly(vinylpyridine) resin towards several metal ions [2].

In the present study, IIP were applied as an adsorbent material for selective recognition of  $\text{Co}^{2+}$  ions from aqueous medium. Cobalt ion was chosen as a target metal ion as it was environmentally toxic and enters the environment mostly from human activities such as industry of mining and pigment [3] plastic and catalytic process [4] alloys industry [5] and many more. It can form both bivalent and trivalent compounds. Human can be exposed to cobalt in variety of pathways such as drinking water, breathing air and food supply. For these reasons, separation of cobalt ion is needed to overcome the excessive exposure towards it. Because of their importance from an environmental viewpoint, numerous methods have been produced in sequestration of cobalt ion from aqueous solution such as salting-out phase separation [6] extraction by almond green hull [7] biosorptive removal [8] solvent extraction [9] and many more.

Therefore, one of the greatly developed techniques for the preparation of metal extraction is by applying the molecular imprinting technology. It is a technique for the preparation of polymeric materials that are capable of molecular recognition for selective separation and chemical analysis, amongst other applications [10]. The application of IIP using cobalt ions as target analyte was investigated as one of the alternative ways to improve any drawbacks of the existing methods and produce a less costly procedure in the extraction of cobalt ions in aqueous media. The imprinting effect of Co-IIP was studied to get the information on adsorption behavior in terms of equilibrium isotherms and kinetic motion of Co-IIP towards  $\text{Co}^{2+}$  ions, which will be extended to further development of technological appliances especially for environmental concern.

## 2. Methodology

### 2.1. Chemicals

Methacrylic acid (MAA), ethylene glycol dimethacrylate (EGDMA), 2,2'-azobisisobutyronitrile (AIBN), methanol, ethylenediaminetetraacetic acid (EDTA), hydrochloric acid (HCl) and dipicolinic acid (DPA) were purchased from Sigma-Aldrich. Cobalt (II) chloride (Hexahydrate) was supplied from Scharlau. All chemicals were purified before use and AIBN was re-crystallized from methanol.

### 2.2. Synthesis of Imprinted Polymers

The IIP was synthesized by bulk polymerization method. The template was first prepared by reacting  $\text{CoCl}_2$  with dipicolinic acid to form a complex before being polymerized with monomer. The  $\text{Co}^{2+}$ -dipicolinate complex, MAA, EGDMA and AIBN was dissolved in 5.00 ml of methanol to allow the polymerization process. The ratio used for template: monomer: cross-linker was 1: 4: 20. The solution was degassed for 10 minutes and then placed in an oil-bath at  $60^\circ\text{C}$  for 24 hours. NIP was prepared in the same manner as controlled polymer but in the absence of  $\text{Co}^{2+}$ -complex. The resultant polymers were then ground and sieved using acetone to obtain the particles with sizes less than  $25\ \mu\text{m}$ . It was then collected after

sedimentation from acetone. The template, unreacted monomers or diluents were leached out *via* continuous stirring with EDTA and HCl in 9:1 ratio for 24 hours. Figure 1 shows the proposed schematic reaction of Co-IIP.

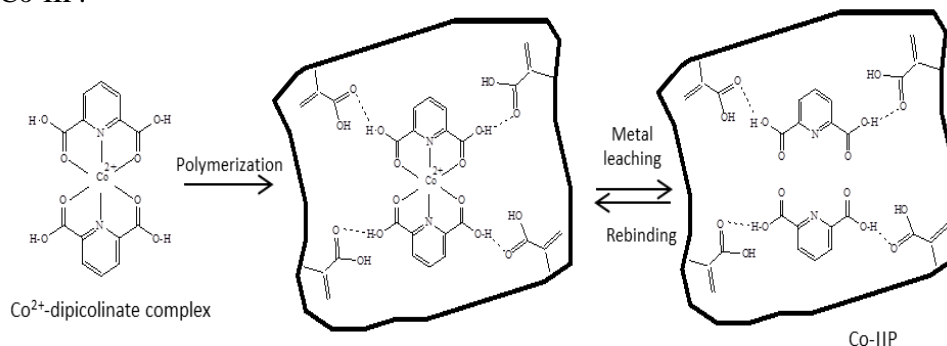


**Figure 1.** Schematic representation of Co-IIP imprinting process.

### 2.3. Characterization Techniques

The surface and morphological properties of IIP and NIP monolith size was characterized using Scanning Electron Microscopy (SEM) model JEOL JSM-6360LA. Samples were prepared and placed on metal stubs and coated with thin layer of Au. The textural characteristic was viewed under 5000x magnification. The chemical structure of the imprinted polymer was determined using Fourier Transformed Infrared (FTIR) spectrometer from Perkin Elmer with spectrum 100 as the software. Attenuated Total Reflectance (ATR) method was used in order to get the FTIR spectra. The spectra were recorded in the range of 4000 to 400  $\text{cm}^{-1}$  wavenumbers.

### 2.4. Binding Studies

Equilibrium batch rebinding experiment were studied using Atomic Absorption Spectroscopy (AAS). 25 ml of 10 ppm of  $\text{Co}^{2+}$  solution was added to the different mass of polymers (1, 5, 10, 11, 12, 13 and 15 mg). Each mixture was shaken for different time (5, 15, 30, 60, 90 and 120 minutes) to facilitate the adsorption of  $\text{Co}^{2+}$  ions onto polymers. After the binding process was complete for predetermined time, the solution was filtered and analyzed by using AAS to identify the concentration of free  $\text{Co}^{2+}$  in solutions. The data obtained was used to study the adsorption properties of Co-IIP and NIP by adsorption isotherm modelling. The adsorption capacity was calculated using the Equation (1).

$$q_e = \frac{(C_i - C_f)V}{W} \quad (1)$$

where  $q_e$  is the amount of  $\text{Co}^{2+}$  adsorbed ( $\text{mg g}^{-1}$ ),  $C_i$  is the initial concentration of  $\text{Co}^{2+}$  ions solution (ppm),  $C_f$  is the final concentration of  $\text{Co}^{2+}$  ions solution (ppm),  $V$  is the volume of  $\text{Co}^{2+}$  ions solution used (L) and  $w$  is the weight of polymer applied to the solution (g).

## 3. Results

### 3.1. Characterization of Polymers

Co-IIP and NIP were successfully synthesized using free radical polymerization. The Co-IIP and NIP were characterized by FTIR analysis. The FTIR spectra for Co-IIP and NIP were recorded as shown in Figure 2, it is obvious that Co-IIP and NIP possessed similar backbone structure. The interaction between template and monomer present in Co-IIP gave changeable peaks from NIP spectrum to Co-IIP spectrum.

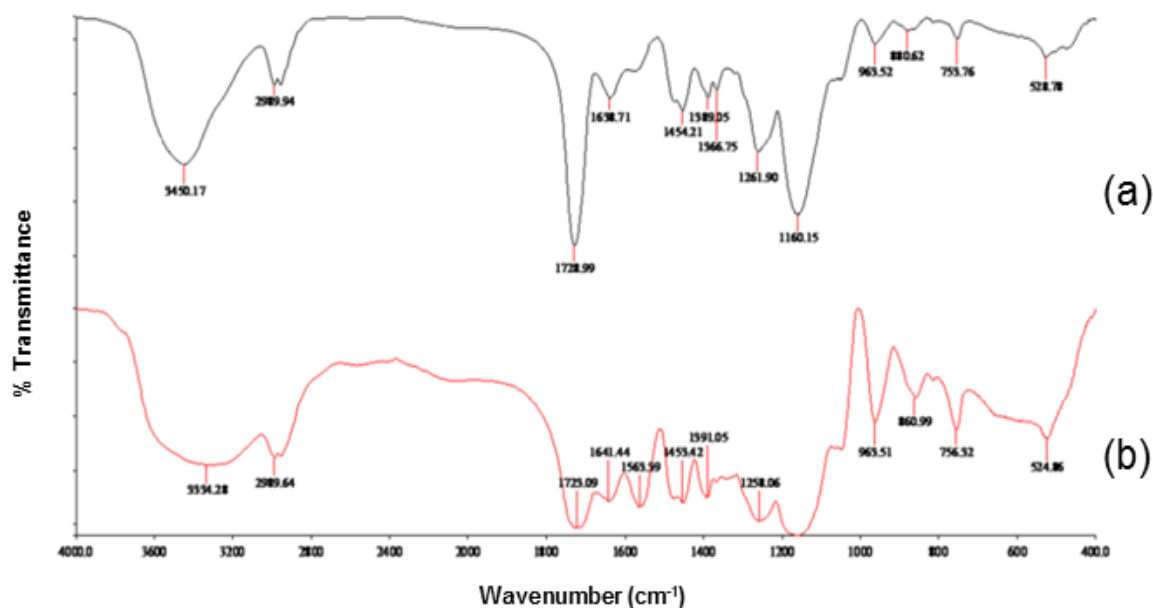


**Figure 2.** FTIR spectra for (a) NIP and (b) Co-IIP.

From bulk polymerization, polymers were obtained in monolith form; irregular shape and size. Particles with size range of 1-25  $\mu\text{m}$  were collected and used in this study. Figure 3 shows the SEM micrographs for Co-IIP and NIP. The surface morphology for Co-IIP was rougher compared to NIP, which was smoother and cleaner surface.

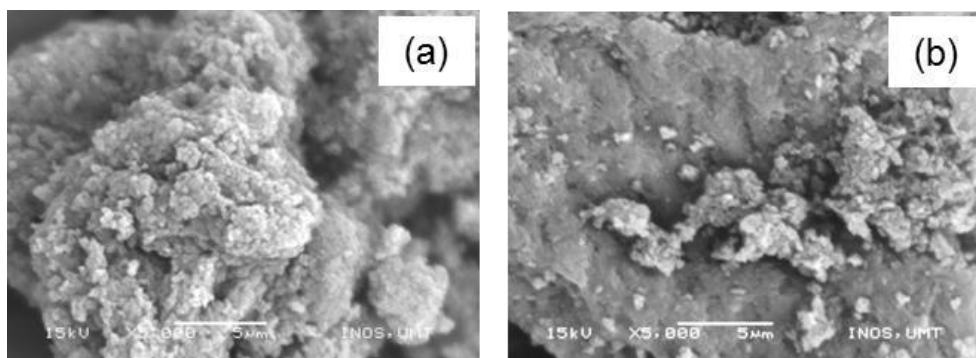


**Figure 3.** SEM micrograph for (a) Co-IIP and (b) NIP.

### 3.2. Adsorption Isotherm

The adsorption isotherm for Co-IIP and NIP were investigated to illustrate the interactive behavior between  $\text{Co}^{2+}$  ions and polymeric cavities. Series of calculation were carried out to investigate the adsorption capacity, as well as describing polymers' surface properties and affinity to  $\text{Co}^{2+}$  ions. For the effect of polymer dosage (Figure 4), it was observed that when the dosage of polymers were increased from 1 mg to 12 mg, the removal efficiency of  $\text{Co}^{2+}$  ions increase as expected. The removal efficiency of Co-IIP increased from 10.13% to 94.94%, as compared to slight increased from 3.58% to 36.66% for NIP.

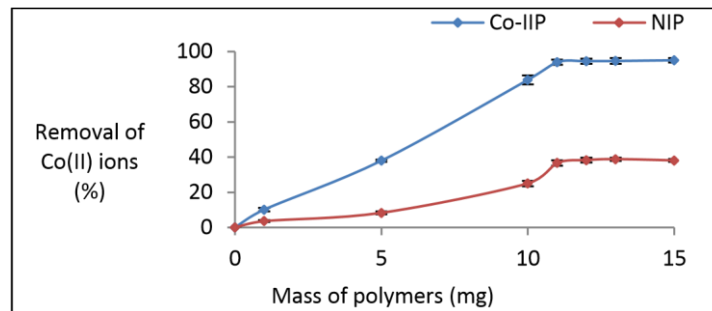


**Figure 4.** Effect of polymers dosage on the adsorption of  $\text{Co}^{2+}$  onto Co-IIP and NIP.

Linearized graphs of Langmuir [11] and Freundlich [12] were produced by fitting all the equilibrium data for both polymers in order to get the applicability of isotherm models. Langmuir model of adsorption is described as the Equation (2).

$$\frac{C_e}{Q_e} = \frac{1}{Q_o} C_e + \frac{1}{Q_o b} \quad (2)$$

where  $C_e$  ( $\text{mg L}^{-1}$ ) is the equilibrium concentration,  $Q_e$  is the adsorption amount at equilibrium ( $\text{mg g}^{-1}$ ),  $Q_o$  is the maximum adsorption capacity ( $\text{mg g}^{-1}$ ) and  $b$  is Langmuir adsorption constants ( $\text{L mg}^{-1}$ ). Langmuir isotherm can be plotted as  $C_e/Q_e$  against  $C_e$ ,  $1/Q_o$  as slope and  $1/Q_o b$  as intercept. The second isotherm model used in this study is Freundlich model and a linear equation can be described as in Equation (3).

$$\log Q_e = \log K_F + \frac{1}{n} \log C_e \quad (3)$$

where  $K_F$  is the Freundlich constant while  $n$  is the Freundlich exponent. Freundlich isotherm can be plotted as  $\log Q_e$  against  $\log C_e$ ;  $\log K_F$  becomes the intercept of the line and  $1/n$  becomes the slope of the line. The constant  $K_F$  indicates adsorption capacity, while  $1/n$  shows the strength of adsorption during adsorption process.

Linearized forms of Langmuir and Freundlich isotherm were plotted as shown in Figure 5 and Figure 6, respectively. It was found that the adsorption of Co-IIP and NIP fitted better with Langmuir isotherm than Freundlich isotherm by given higher correlation coefficient,  $R^2$  values. Therefore, it can be concluded that the sorption of  $\text{Co}^{2+}$  ions by Co-IIP and NIP were followed the Langmuir isotherm model. The information on isotherm parameter was calculated from the straight line equation and tabulated in Table 1.

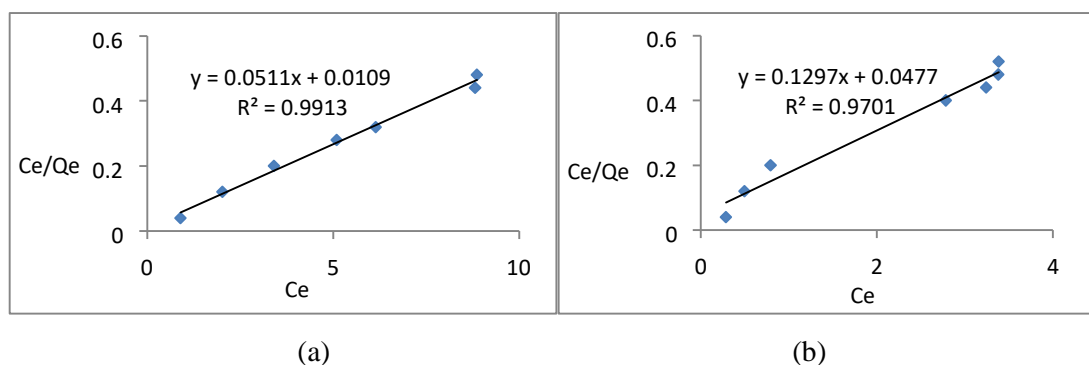


**Figure 5.** Langmuir plot for adsorption of  $\text{Co}^{2+}$  ions by (a) Co-IIP and (b) NIP.

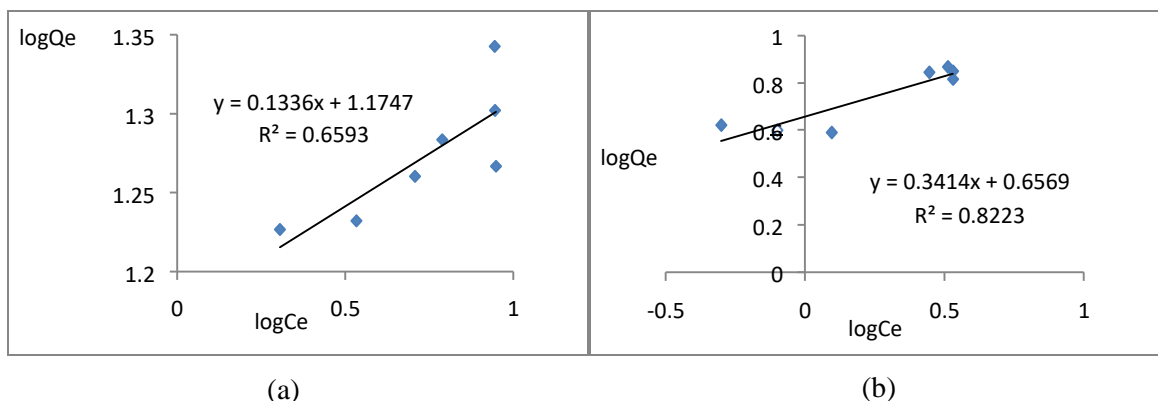


**Figure 6.** Freundlich plot for adsorption of  $\text{Co}^{2+}$  by (a) Co-IIP and (b) NIP.

The separation factor,  $R_L$  is a dimensionless constant was calculated to understand the essential features of the Langmuir equation by using Equation (4).

$$R_L = \frac{1}{1 + bC_o} \tag{4}$$

where  $C_o$  is initial concentration of  $\text{Co}^{2+}$  solution and  $b$  is the Langmuir constant.  $R_L$  indicates the nature adsorption of Co-IIP and NIP. The adsorption process is unfavorable if  $R_L > 1$ , linear if  $R_L = 1$ , favorable if  $0 < R_L < 1$  and irreversible if  $R_L = 0$  [13, 14]. Result obtained for Co-IIP and NIP in this study showed that  $R_L$  values were in the range of favorable.

**Table 1.** Isotherm constant for Co-IIP and NIP.

Polymers	$Q_o$ ( $\text{mg g}^{-1}$ )	Langmuir			Freundlich			
		$b$ ( $\text{Lmg}^{-1}$ )	$R_L$	$R^2$	$1/n$ ( $\text{mg g}^{-1}$ )	$n$ ( $\text{L mg}^{-1}$ )	$K_F$ ( $\text{mg g}^{-1}$ )	$R^2$
Co-IIP	19.56	4.68	0.0208	0.99	0.13	7.48	0.07	0.65
NIP	7.41	4.17	0.0233	0.97	0.34	2.92	4.53	0.82

### 3.3. Kinetic Studies

The adsorption kinetic was studied to describe the underlying mechanism of the adsorption process and the rate at which  $\text{Co}^{2+}$  ions are adsorbed onto the surface of polymers. The adsorption capacity curves of Co-IIP and NIP was illustrated as shown in Figure 7. As it can be seen, the adsorption process involved two stages. Initially, the adsorption rate was rapid increase for the first 30 minutes with an adsorption capacity of  $8.86 \text{ mg g}^{-1}$  and  $3.38 \text{ mg g}^{-1}$  for Co-IIP and NIP respectively. Then, after 30 minutes, adsorption rate remained constant and achieved equilibrium state because of the saturation of polymeric matrices occupied by  $\text{Co}^{2+}$  ions. Co-IIP showed much higher adsorption capacity as compared with NIP. Therefore, the Co-IIP was said to perform more efficient than NIP in adsorbing  $\text{Co}^{2+}$  ions. The equilibrium data were analyzed using pseudo-first-order and pseudo-second-order rate model. Results were obtained in triplicate analysis with errors based on  $\pm 1$  standard deviation.

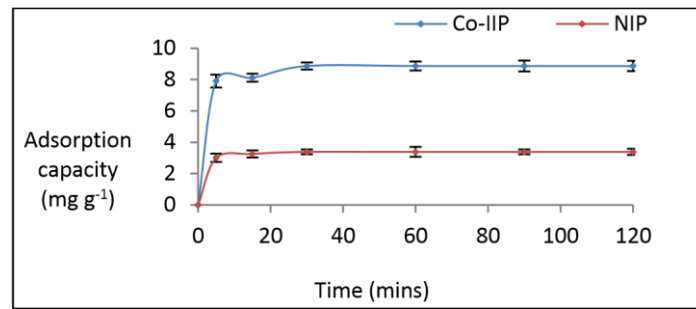


**Figure 7.** Adsorption capacity of  $\text{Co}^{2+}$  by Co-IIP and NIP.

The kinetic equation of pseudo-first-order represent as in Equation (5) [15].

$$\ln(q_e - q_t) = \ln q_e - k_1 t \quad (5)$$

where  $k_1$  is the adsorption rate constant of pseudo-first-order kinetic ( $\text{min}^{-1}$ ),  $t$  is the contact time between adsorbate and adsorbent, while  $q_e$  and  $q_t$  are the amount of  $\text{Co}^{2+}$  ions adsorbed at equilibrium and at any time ( $\text{mg g}^{-1}$ ) respectively. Meanwhile, pseudo-second order kinetic model was described by using the kinetic Equation (6) [16].

$$\frac{t}{q_t} = \frac{k_2}{h} + \frac{t}{q_e} \quad (6)$$

where  $h = k^2 q_e^2$  is the initial adsorption rate, while  $k_2$  is the pseudo-second-order rate constant. The parameter  $q_e$  here is referred as  $q_{e,cal}$  to show the calculated amount of  $\text{Co}^{2+}$  ions adsorbed at equilibrium from the plotted graphs.

In order to ensure the suitability of kinetic models of polymers, both normalized standard deviation value,  $\Delta q$  (%) and relative errors (%) were calculated as described as the equations below.

$$\Delta q(\%) = \sqrt{\frac{[(q_{e,exp} - q_{e,cal})/q_{e,exp}]^2}{N - 1}} \times 100\% \quad (7)$$

$$Relative\ error\ (\%) = \frac{|q_{e,cal} - q_{e,exp}|}{q_{e,exp}} \times 100\% \quad (8)$$

where  $N$  is the amount of data points fitted to the plot,  $q_{e,exp}$  and  $q_{e,cal}$  ( $\text{mg g}^{-1}$ ) are the experimental and calculated adsorption capacity respectively. The lower  $\Delta q$  (%) gives best fitness of polymer to the kinetic model.

The graphs for pseudo-first-order and pseudo-second-order were plotted (Figure 8 and Figure 9, respectively) and the parameters were calculated as shown in Table 2. The kinetic of adsorption exhibited by  $\text{Co}^{2+}$  ion as divalent metallic ion was described by pseudo-second-order kinetic by give higher  $R^2$  values for both polymers.

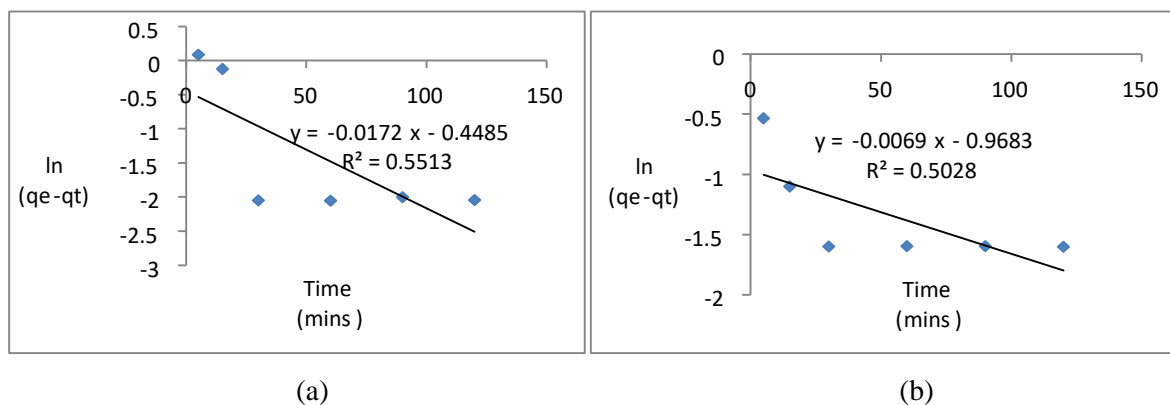


**Figure 8.** Pseudo-first-order plots for adsorption of  $\text{Co}^{2+}$  ions by (a) Co-IIP and (b) NIP.

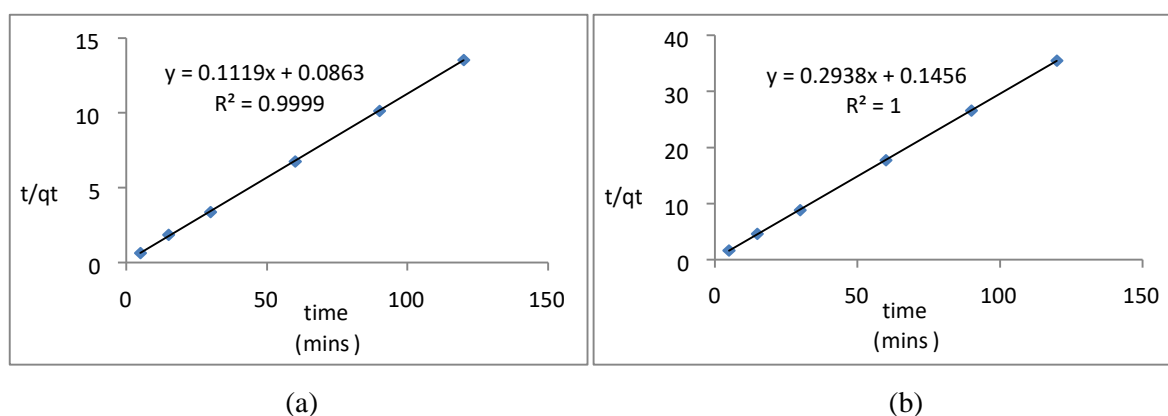


**Figure 9.** Pseudo-second-order plots for adsorption of  $\text{Co}^{2+}$  ions by (a) Co-IIP and (b) NIP.

**Table 2.** Kinetic constant for Co-IIP and NIP.

Polymer	Pseudo-first-order					Pseudo-second-order					
	$q_{e,cal}$ ( $\text{mg g}^{-1}$ )	$k_1$	$R^2$	$\Delta q$ (%)	RE (%)	$q_{e,cal}$ ( $\text{mg g}^{-1}$ )	$k_2$	$h$ ( $\text{g.min mg}^{-1}$ )	$R^2$	$\Delta q$ (%)	RE (%)
Co-IIP	0.63	0.0172	0.55	41.50	92.7 9	8.93	0.14	11.58	0.99	0.34	0.76
NIP	0.37	0.0069	0.50	39.78	88.7 8	3.40	0.59	6.86	1.00	$5.31 \times 10^{-4}$	0.54

#### 4. Discussion

For FTIR analysis, as expected for the similar backbone FTIR structure was due to the same monomers were used in the production of the polymers [17] and high level of cross-linking agent used. Based on Figure 2, a few peaks was shifted from NIP to Co-IIP; for example, the O-H stretching band shifted from  $3450 \text{ cm}^{-1}$  to  $3334 \text{ cm}^{-1}$ , C=O stretching band shifted from  $1728 \text{ cm}^{-1}$  to  $1723 \text{ cm}^{-1}$  and C-O stretching band shifted from  $1160 \text{ cm}^{-1}$  to  $1161 \text{ cm}^{-1}$ . These shifted peaks can be reasoned of the formation of dative bond between  $\text{Co}^{2+}$  ion and dipicolinic acid. Co-IIP exhibited a relatively rougher surface due to the imprinting effect of  $\text{Co}^{2+}$  ions onto the surface, which resulted in cavities compared

to NIP. IIP with rougher surfaces also facilitates the mass transfer rate of metal ions toward the polymer surface and consequently improves its adsorption capacity [18].

For the adsorption study, the higher performance of Co-IIP could be reasoned by the possession of specific cavities to allow the adsorption of  $\text{Co}^{2+}$  ions onto the surface, as in agreement with SEM images showed slightly rougher surface in Co-IIP compared to NIP. The further increase in dosage of Co-IIP and NIP after 12 mg produced almost plateau values which indicated that equilibrium was achieved. This could be attributed to saturation of cavities for both polymers. Results based on average values for triplicate analysis with error based on  $\pm 1$  standard deviation.

The equilibrium data obtained was found to be appropriate towards the Langmuir isotherm. This isotherm assuming that the recognition sites of outer surface of adsorbent are homogeneous and the adsorbate is adsorbed at well-defined sites, leading to monolayer coverage of the adsorbate surface. Thus, this can be assumed that  $\text{Co}^{2+}$  ions were adsorbed at a fixed number of well-definite recognition cavities which each cavity can only uptake one  $\text{Co}^{2+}$  ions. These cavities are considered energetically equivalent and there is a distance between cavities to ensure that no interaction between adsorbed  $\text{Co}^{2+}$  ions to adjacent sites [19].

The maximum adsorption capacity,  $Q_o$  obtained (Table 1) from Langmuir isotherm for Co-IIP was 2.6 times higher than NIP, with the value of  $19.56 \text{ mg g}^{-1}$  and  $7.41 \text{ mg g}^{-1}$  respectively. This proved the presence of high amount of microspores with higher specificity and affinity on the Co-IIP surface than NIP, allowing more amounts of  $\text{Co}^{2+}$  ions adsorbed into the cavities. The maximum adsorption capacity (experimental) obtained for Co-IIP and NIP was  $18.47 \text{ mg g}^{-1}$  and  $3.58 \text{ mg g}^{-1}$  respectively. Thus, the values calculated,  $Q_o$  for Langmuir isotherm model is comparable to the experimental values.

In the pseudo-second-order theory, the rate-limiting step is chemisorption process between  $\text{Co}^{2+}$  ions and cavities. This process involves the valence force that allows the exchange or sharing of electrons to occur. With response to this research,  $\text{Co}^{2+}$  ions can interact with two types of adsorption cavities, either  $\text{Co}^{2+}$  ions was imprinted by active sites in the polymers or they can result in the formation of inclusion complex with functional monomers, (MAA) during the molecular recognition stage (Wang et al., 2011). The adsorption rate of  $\text{Co}^{2+}$  ions onto the cavities was evaluated by looking at the initial adsorption rate,  $h$ . Co-IIP was found to be faster in adsorbing  $\text{Co}^{2+}$  ions relative to NIP with the initial adsorption rate of  $11.58 \text{ g.min mg}^{-1}$ , which was 1.7 times faster than NIP (Table 2).

The accuracy and validity of kinetic models were further compared with normalized standard deviation value ( $\Delta q$ ) and percentage relative errors (RE) to strengthen the data that both polymers are follows pseudo-second order kinetic model. The value of  $q_{e,exp}$  obtained for Co-IIP and NIP were 8.86 and  $3.38 \text{ mg g}^{-1}$  respectively. Both polymers fitted better to pseudo-second-order as the difference between  $q_{e,cal}$  and  $q_{e,exp}$  was small. This model also showed the relatively low for  $\Delta q$  and RE value as compared to pseudo-first-order kinetic model.

## 5. Conclusion

The potential of Co-IIP for the effective removal of  $\text{Co}^{2+}$  ions was successfully demonstrated. It has been shown that Co-IIP showed better performance than NIP by successfully adsorbing 94%  $\text{Co}^{2+}$  ions in the aqueous solution. Batch rebinding experiment were revealed that the adsorption isotherm was followed Langmuir isotherm which produce the homogenous polymer surface. For kinetic study, pseudo-second-order kinetic models was successfully fit the data thus revealed the chemisorption process occurred in the system.

## 6. References

- [1] Komiyama M, Takeuchi T, Mukawa T and Asanuma H 2003 *Molecular Imprinting: from fundamentals to applications* (Wiley-VCH Verlag GmbH & Co. KGaA) p i-xii
- [2] Nishide H, Deguchi J and Tsuchida E 1977 *Journal of Polymer Science: Polymer Chemistry Edition* **15** 3023-3029

- [3] Faroon O, Abadin H, Keith S, Osier M, Chappell L, Dimond G and Sage G 2004 Toxicological profile for cobalt. US Department of Health and Human Services AFTSaDR, Atlanta: Agency for Toxic Substances and Disease Restistry
- [4] Khodakov A Y, Chu W and Fongarland P 2007 *Chemical Reviews* **107** 1692-1744
- [5] Guo W, Chen R, Liu Y, Meng M, Meng X, Hu Z and Song Z 2013 *Colloids and Surfaces A: Physicochemical and Engineering Aspects* **436** 693-703
- [6] Habib A, Wahiduzzaman M, Rashid H -O, Islam A, Ferdoushi F K and Alam A S 2008 *Pakistan Journal of Analytical Environment Chemistry* **9** 6-10
- [7] Ahmadpour A, Tahmasbi M, Bastami T R and Besharati J A 2009 *Journal of Hazardous Materials* **166** 925-930
- [8] Egila J, Dauda B and Jimoh T 2010 *African Journal of Biotechnology* **9** 8192-8198
- [9] Lee M, Kim S, Choi Y and Chae J 2011 *Materials Transaction* **52** 1211-1215
- [10] Mehamod F S, KuBulat K, Yusof N F and Othman N A 2015 *International Journal of Technology* **4** 546-554
- [11] Sime R J 2000 *Infohost. Nmt. Edu* **7**
- [12] Mittal A, Kurup L and Mittal J 2007 *Journal of Hazardous Materials* **146** 243-248
- [13] Malkoc E and Nuhoglu Y 2007 *Separation and Purification Technology* **54** 291-298
- [14] Sathish T and Vinithkumar N V 2015 *Applied Water Science* **5** 153-160
- [15] Yuh-Shan H 2003 *Scientometrics* **59** 171-177
- [16] Ho Y S and McKay G 1999 *Process Biochemistry* **34** 451-465
- [17] Othman N A, Daik R, Suah F B M and Mehamod F S 2016 *International Journal of Applied Chemistry* **12** 661-674
- [18] Yilmaz V, Arslan Z, Hazer O and Yilmaz H 2014 *Microchemical Journal* **114** 65-72
- [19] Yavuz H, Say R and Denizli A 2005 *Materials Science and Engineering C* **25** 521-528

### **Acknowledgment**

We would like to thank for Ministry of Higher Education Malaysia for project funding supported under Fundamental Research Grant Scheme (FRGS-Vote No. 59263).